

Present and future of neutrino oscillation experiments

A. Ereditato

INFN Napoli, Italy

Received: 17 Dec 2001 / Accepted: 15 Mai 2002 / Published online: 25 Sep 2002

Abstract. The possibility of a non-vanishing neutrino mass is an intriguing question in the present scenario of particle physics. On the one hand, there are no fundamental principles for the neutrino to be massless; on the other hand, a massive neutrino would indicate the existence of physics beyond the Standard Model of the elementary particles, hence representing a fundamental milestone in particle physics. In this paper a picture of the present experimental situation of massive neutrino physics is outlined focusing on the strong experimental indications for neutrino oscillation. Emphasis is given to the future project aiming at the clarification of the scenario and to the assessment of the oscillation hypothesis. Future experiments will make use of neutrinos from astrophysics sources, from the Sun, from the atmosphere and from nuclear reactors and particle accelerators: it would be very hard to make an exhaustive review of these many experimental attempts. Therefore, I will only concentrate on (some!) solar, atmospheric and long baseline (LBL) accelerator neutrino projects and to their impact on the understanding of the neutrino mixing matrix.

PACS: not given

1 Our present knowledge about neutrinos

The main new facts contributing to our present knowledge on neutrino physics can be schematically summarized as follows:

- Experiments on the direct measurement of the neutrino mass and those searching for neutrino less double decay have yielded so far negative results. Kinematical methods based on Tritium beta decay have been used by the Mainz and Troisk groups [1] to set limits on the ν_e mass of about $2 eV$ at the 95% C.L. From the study of pion decay limits of $\sim 190 eV$ for the ν_μ mass have been set, largely dominated by uncertainties on the value of the pion mass. Finally, high-energy LEP experiments have determined limits of $\sim 15 - 16 MeV$ for the ν_τ mass by studying kinematical correlation in multi-pion τ decays.

Double beta 'two-neutrino' decay has been observed by radio chemical inclusive methods. However, only limits have been set by direct counting experiments searching for the neutrino-less decay that can only take place for massive neutrinos. The present limits on the neutrino mass of $\sim 1 eV$ are affected by theoretical uncertainties in the matrix element calculations.

- Three neutrino species have been directly observed. The Fermilab DONUT experiment [2] has identified candidate events for the production and decay of τ leptons from ν_τ charged current interactions. This represents the first direct evidence for the existence of the ν_τ . In DONUT neutrinos originate from a beam dump of 800 GeV protons hitting an emulsion target complemented by electronic tracking detectors. The target design is based on the so called Emulsion Cloud Chamber technique, recently revised for the large scale OPERA detector searching for $\nu_\mu \rightarrow \nu_\tau$ oscillations [3]. The analysis of the emulsions profits today from the impressive advances in the modern automatic scanning devices which make use of high-speed computer-controlled microscopes.
- There is a $\sim 10 \sigma$ evidence for the disappearance of atmospheric ν_μ . The observed deficit of ν_μ produced in the atmosphere by cosmic rays and its zenith angle dependence as measured by the Super-Kamiokande experiment [4] strongly favors the hypothesis of neutrino oscillation.
- There is a $\sim 3 \sigma$ evidence for the conversion of solar ν_e into another (active) neutrino flavor. The detected solar ν_e flux is about a factor two smaller than that predicted by the so called Standard Solar Model (SSM) [5]. The results from the SNO experiment [6] combined with the measurement by Super-Kamiokande have shown at the three sigma level that the oscillation scenario is favored and that the SSM is correct.
- Neutrino oscillation can explain both the solar and the atmospheric neutrino deficit. Concerning the oscillation parameters, small Δm^2 and large mixing angles seem to be favorite in a three-flavor mixing scheme without sterile neutrinos.
- The existence of neutrino oscillation implies massive neutrinos and therefore the first compelling evidence of physics beyond the minimal Standard Model.

2 The Solar Neutrino Problem and its solution

Electron neutrinos are produced in the thermonuclear reactions occurring inside the Sun. Each reaction is characterized by a specific energy spectrum of the emitted neutrinos. The spectra can be predicted by theory and are graphically shown in Fig. 1.

The first experimental observation made with solar neutrinos and compatible with the hypothesis of neutrino oscillation originated from a discrepancy between the measured detection rate in the solar neutrino experiment by R. Davis [7] and the theoretical calculations [5]: a statistically significant deficit in the measured flux of ν_e was observed. This effect is commonly referred to as the *solar neutrino problem*. Although solutions questioning our understanding of the Sun have been contemplated, it seems now that the deficit can be interpreted by assuming that electron neutrinos oscillate into a different flavor in their travel towards the Earth. So far, five different experiments confirmed and consolidated the measurement of the solar neutrino deficit.

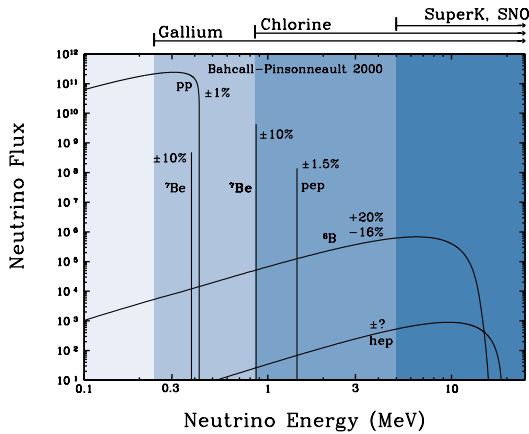


Fig. 1. Predicted spectrum of solar neutrinos [5]. Neutrino fluxes from continuum sources (such as pp and 8B) are given in $cm^{-2}s^{-1}MeV^{-1}$. Those from discrete sources (such as 7Be) are given in $cm^{-2}s^{-1}$. Also shown are the thresholds for the different reactions used for neutrino detection

The Davis experiment was based on the radio chemical Chlorine technique and has been running in the Homestake Gold mine in South Dakota for about 30 years. The apparatus consisted of 615 *ton* of C_2Cl_4 and allowed the detection of solar ν_e through the inverse β -decay reaction $\nu_e + {}_{17}^{37}Cl \rightarrow {}_{18}^{37}Ar + e^-$. The energy threshold for this process is $E_\nu = 0.813 MeV$ and it is just below the $0.862 MeV$ 7Be line. Therefore, the detected neutrino flux is mainly due to 7Be and 8B reactions. The experimental detection method exploits the electron capture reaction ${}_{18}^{37}Ar + e^- \rightarrow {}_{17}^{37}Cl + \nu_e + X_{rays}$. The measured capture rate corresponds to $2.56 \pm 0.16 \pm 0.16 SNU$ (Solar Neutrino Unit) while the predicted flux is $7.7_{-1.0}^{+1.2} SNU = 0.0(pp) + 0.2(pep) + 1.15({}^7Be) + 5.9({}^8B) + 0.5(CNO)$. The disagreement between predictions and measurements is statistically significant (more than 3.5σ).

Another category of radio chemical experiments makes use of Gallium instead of Chlorine in order to profit from the lower energy threshold ($0.233 MeV$) of the reaction $\nu_e + {}_{31}^{71}Ga \rightarrow {}_{32}^{71}Ge + e^-$. These experiments are therefore sensitive to the pp component of the solar neutrino spectrum. The luminosity of the Sun is mainly determined by the pp chain and is a well measured quantity. This constraint affects positively the prediction of the solar neutrino flux coming from the pp reaction. Three Collaborations performed this experiment: GALLEX and the follow-up GNO [8], and SAGE [9]. GNO is now running underground in the Gran Sasso Laboratory and will eventually make use 100 *ton* of Gallium. SAGE was placed in the laboratory under Mount Andryrchi and used 60 *ton* of Gallium. The ${}_{32}^{71}Ge$ atoms are detected through the capture reaction ${}_{32}^{71}Ge + e^- \rightarrow {}_{31}^{71}Ga + \nu_e + X_{rays}$. The predicted solar neutrino flux is $129_{-7}^{+9} SNU = 69.6(pp) + 2.8(pep) + 34.4({}^7Be) + 12.4({}^8B) + 9.8(CNO)$, and it has to be compared with the rates measured by GALLEX/GNO and SAGE,

Table 1. Results from solar neutrino experiment normalized to theoretical predictions

Experiment	Result/Theory
Homestake	0.33 ± 0.03
GALLEX/GNO	0.57 ± 0.06
SAGE	0.58 ± 0.06
Kamiokande	0.54 ± 0.08
Super-Kamiokande	0.45 ± 0.02
SNO	0.35 ± 0.03

respectively of $74_{-6}^{+7} SNU$ and $75.2_{-7}^{+8} SNU$. Also in this case the disagreement between predicted and measured flux is at the level of 3.5σ .

A third technique exploited for the detection of solar neutrinos is the one originally adopted by the Kamiokande experiment and with higher statistics by the follow-up Super-Kamiokande detector [4]. The latter is located in the Kamioka Underground Laboratory. The laboratory has an elevation of $350 m$ with a rock overburden of about $1000 m$ in the vertical direction. Super-Kamiokande is a cylindrical large ring-imaging water Cerenkov detector with a volume of $50000 m^3$. It detects the light emitted by relativistic charged particles in water by means of PMTs arrayed in two dimensions on the detector inner walls. A Cerenkov ring image (which corresponds to a single charged particle above threshold) is projected onto the detector walls covered by ~ 11000 photo-multipliers. In the Super-Kamiokande terminology a single (multi) ring event corresponds to a quasi-elastic (deep-inelastic) interaction.

Results from 1258 days of data taking have been presented. For their analysis a fiducial volume of $22.5 kton$ and an energy threshold of $\sim 5 MeV$ are used. The measured flux is $(2.32 \pm 0.03 \pm 0.07) \times 10^6 cm^{-2}s^{-1}$ and corresponds to $\sim 45\%$ of the expected flux. The results of Super-Kamiokande and of other solar neutrino experiments are summarized in Table 1, normalized to the theoretical predictions.

Super-Kamiokande also reported on the evaluation of a possible day-night dependence of the event yield, which is expected if neutrino oscillation is the explanation of the solar neutrino deficit. Neutrinos oscillated in the Sun (ν_μ or ν_τ) could re-convert inside the Earth into the original ν_e flavor. This effect would lead to a higher rate of detected ν_e during the night. The measured day-night asymmetry is $(N - D)/0.5 \times (D + N) = 0.033 \pm 0.022 \pm 0.013$. The signal significance is still too small to confirm the effect.

The distortion of the neutrino energy spectrum is another feature that can be related to neutrino oscillation. The shape of the spectrum determines the energy distribution of the recoil electron produced in the $\nu_e - e$ interaction. Departure from the predictions of the electroweak theory would be indication of new physics. The fit to the data on the recoil energy spectrum obtained assuming the undistorted spectrum is only marginally acceptable. Unfortunately, the statistical and systematic errors are still too large to draw firm conclusions.

Recently, the beautiful result from the SNO experiment [6] has contributed to the clarification of the scenario, strongly pointing to the interpretation of the solar neutrino deficit in terms of oscillation of electron neutrinos into another active flavor. The detector is located in the Sudbury underground laboratory and consists of 1000 *ton* of a heavy water (D_2O) target viewed by about 9500 PMTs. The detection method is similar to that of Super-Kamiokande. However, the use of heavy water allows the detection of three kinds of neutrino interactions

$$\nu_e + d \rightarrow p + p + e^- \quad (\text{charged current})$$

$$\nu_x + d \rightarrow p + n + \nu_x \quad (\text{neutral current})$$

$$\nu_x + e^- \rightarrow \nu_x + e^- \quad (\text{elastic scattering})$$

The first reaction (*CC*) provides a good measurement of the ν_e energy spectrum and has a rather weak directional sensitivity; the second process (*NC*) allows to measure the total 8B neutrino flux from the Sun and features equal cross section for all neutrino species; the third reaction (*ES*) is mainly sensitive to ν_e and (to a smaller extent) also to ν_μ and ν_τ , and has a strong sensitivity to the direction of the incoming neutrino.

The comparison between the above different processes, which can be experimentally distinguished by means of their kinematical features, give selective information on the fluxes of the different neutrino species. In particular, two methods can be applied

$$\frac{CC}{NC} = \frac{\nu_e}{\nu_e + \nu_\mu + \nu_\tau}$$

and

$$\frac{CC}{ES} = \frac{\nu_e}{\nu_e + 0.14(\nu_\mu + \nu_\tau)}$$

The first one has the advantage to directly provide the total neutrino flux and to allow for the cancellation of uncertainties in the cross sections. The second method has been applied so far by the Collaboration; it profits of the fact that ES events point to the direction of the Sun and that one can use the Super-Kamiokande precise measurement of the ES reaction. The result is (in units of $10^6 \text{ cm}^{-2} \text{ s}^{-1}$)

$$\Phi_{SK}^{ES} - \Phi_{SNO}^{CC} = 0.57 \pm 0.17$$

This indicates with a 3.3σ statistical significance the appearance in the solar neutrino flux of active neutrino species different from the original ν_e , excluding at the same time the possibility of a pure $\nu_e \rightarrow \nu_{sterile}$ oscillation and confirming the correctness of the SSM predictions. The measured 8B flux amounts to $(5.44 \pm 0.99) \times 10^6 \text{ cm}^{-2} \text{ s}^{-1}$, in good agreement with the predictions of the SSM of $(5.05_{-0.8}^{+0.1}) \times 10^6 \text{ cm}^{-2} \text{ s}^{-1}$.

The measurements of the solar neutrino flux clearly shows a disagreement with the theoretical predictions, which can be reconciled by assuming neutrino oscillation. A first option contemplates neutrino oscillation in vacuum. Due to the large Sun-Earth distance and to the low energy of solar neutrinos, oscillation with $\Delta m^2 \sim 10^{-11} \text{ eV}^2$ has to be advocated. A second scheme solves the solar neutrino problem by invoking the MSW matter effect [10]. The latter effect

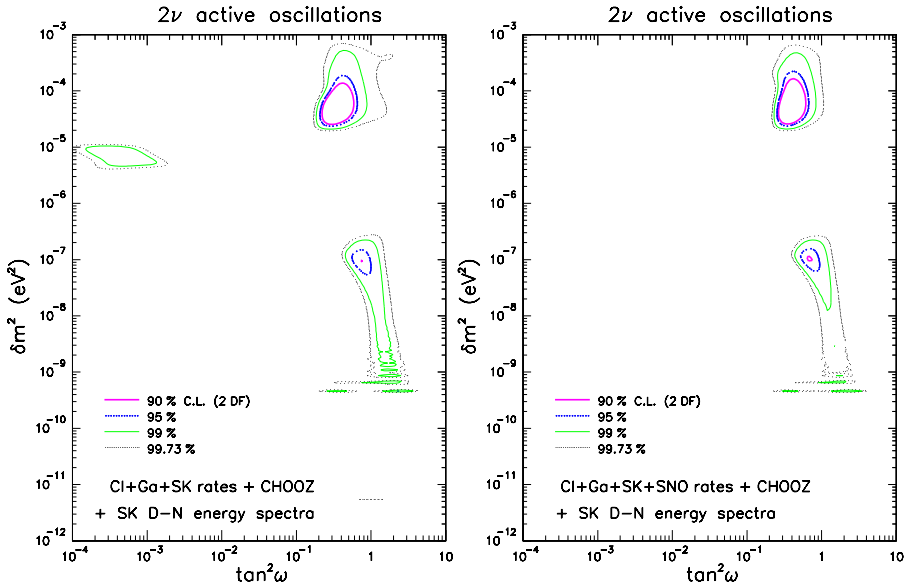


Fig. 2. Oscillation parameters allowed by solar neutrino experiments and by the CHOOZ reactor experiment. Left (right) is without (with) taking into account the SNO results

explains the solar neutrino deficit as a result of the ν_e conversion into ν_μ or ν_τ in the dense solar matter. It is basically due to the fact that ν_e , unlike ν_μ and ν_τ , may undergo both NC and CC interactions with the electrons of the solar matter. In the oscillation of ν_e into another flavor an additional term is introduced in the matrix describing the flavor evolution.

A combined fit of all available solar neutrino experiments [11] provides allowed regions in the $\Delta m^2 - \sin^2 2\theta$ plane as shown in Fig. 2. In the right plot the SNO data have been included in the fit: the result is that large mixing angle (LMA) solutions tend to be preferred.

3 Atmospheric neutrinos

Atmospheric neutrinos are produced by primary cosmic rays interacting with the atmosphere and creating a large number of secondary π and K mesons, mainly with energies of a few GeV . Due to the low density of the atmosphere essentially all the mesons decay before interacting: $\pi/K \rightarrow \mu + \nu_\mu(\bar{\nu}_\mu)$. Most of the muons decay before reaching the ground: $\mu \rightarrow e + \nu_e(\bar{\nu}_e) + \bar{\nu}_\mu(\nu_\mu)$. If all muons decayed one would expect $N(\nu_\mu)/N(\nu_e) = 2$ (ignoring the distinction between ν and $\bar{\nu}$) with $N(\nu_\mu)/N(\nu_e)$ indicating the number of events induced by muon (electron) neutrinos. However, because of the relativistic boost, high energy muons may have not time to decay and therefore a lower value of the ratio is therefore at high energies.

The absolute atmospheric neutrino flux is known [12] with an error of 20–30% essentially due to the uncertainty in the absolute flux of the primary cosmic rays. The error decreases ($\sim 5\%$) for the ratio $(\nu_\mu + \bar{\nu}_\mu)/(\nu_e + \bar{\nu}_e)$. This is the main reason for the commonly used double ratio

$$R = \left(\frac{\mu}{e}\right)_{DATA} / \left(\frac{\mu}{e}\right)_{MC}$$

where μ and e represent the number of μ -like and e -like detected events for real and simulated neutrino interactions, respectively. In the absence of physics beyond the Standard Model one would expect $R = 1$.

The distance L traveled by neutrinos before reaching the detector is related to the zenith angle θ_z through the formula

$$L = \sqrt{R_\oplus^2 + (R_\oplus - d)^2(1 - \cos^2 \theta_z)} - (R_\oplus - d) \cos \theta_z$$

where R_\oplus is the Earth radius ($\sim 6000 \text{ km}$) and d is the average production height ($\sim 10 \text{ km}$). If the deviation of R from unity is due to neutrino oscillation one should expect it varying as a function of the neutrino path length L . Neutrinos produced in interactions above the detector are called *downward-going* and have a typical path length of $\sim 10 \text{ km}$. Neutrinos produced on the opposite side of the Earth are defined *upward-going* and have a path length up to 12000 km . This length may be expressed in terms of $\cos \theta_z$. Neutrino oscillation could therefore be identified by detecting the zenith angle dependence of R . The Super-Kamiokande experiment has proven with large statistical significance this dependence making a strong claim for the observation of neutrino oscillation [4]. In agreement with the result of the reactor experiment CHOOZ [13], no anomaly has been observed for ν_e .

The events in Super-Kamiokande are subdivided in two classes: fully contained (FC) and partially contained (PC) events. For FC events the visible energy is deposited in the fiducial volume of the detector. Conversely, PC events have at least one detected particle exiting the fiducial volume. FC events are further subdivided into *sub-GeV* ($E_{vis} < 1.33 \text{ GeV}$) and *multi-GeV* ($E_{vis} > 1.33 \text{ GeV}$) samples. For PC events no single-ring requirement is made.

The distributions of electron-like and muon-like events as a function of $\cos \theta_z$ are shown in Fig. 3 for various types of contained events and for upward muons produced by ν_μ and $\bar{\nu}_\mu$ interacting with the rock surrounding the detector. A fit assuming $\nu_\mu \rightarrow \nu_\tau$ oscillation is performed and explains well all the measured distributions. The best fit including all classes of events gives the values $\Delta m^2 = 2.4 \times 10^{-3} \text{ eV}^2$ and $\sin^2 2\theta = 1$ constraining the oscillation parameters at the 90% C.L. in the region with $\sin^2 2\theta > 0.88$ and with Δm^2 ranging from $1.3 \times 10^{-3} \text{ eV}^2$ to $5 \times 10^{-3} \text{ eV}^2$. The possibility of $\nu_\mu \rightarrow \nu_{sterile}$ oscillation is contemplated but it is disfavored at the 3σ level.

The SOUDAN2 experiment which makes use of a 1 kton fine-grained tracking calorimeter for the detection of atmospheric neutrinos also observes a smaller than expected R value but with a less pronounced zenith dependence [14] than Super-Kamiokande. Although with low statistics, SOUDAN2 has a better angular resolution than Super-Kamiokande. The best fit to the L/E distribution

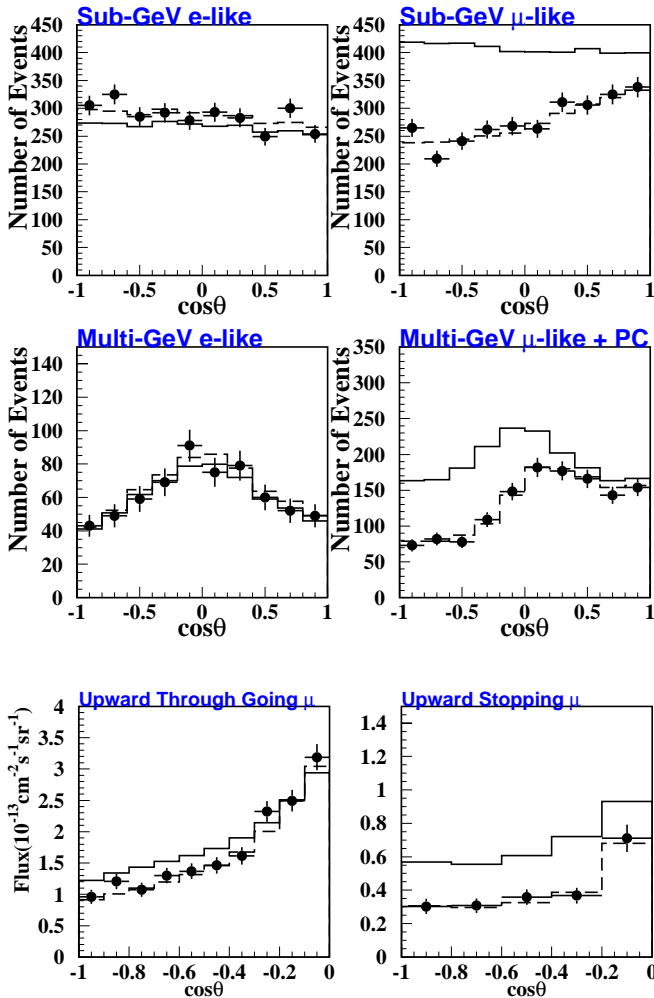


Fig. 3. Zenith angle dependence of various classes of Super-Kamiokande atmospheric neutrino events. The fit parameters are given in the text

gives oscillation parameters $\Delta m^2 = 8 \times 10^{-3} \text{ eV}^2$ and $\sin^2 2\theta = 0.95$. An analysis of the zenith angle dependence has also been performed by the MACRO experiment at the Gran Sasso Laboratory [15] which makes use of a massive calorimeter. The best fit to the L/E distribution gives oscillation parameters consistent with the Super-Kamiokande results.

Super-Kamiokande has also performed a search for atmospheric ν_τ . The expected rate of such events is low: $\sim 1/(k\text{ton} \times \text{year})$, since a ν_τ must have an energy higher than about 3 GeV in order to produce a τ via charged current. Various kinematical methods have been used, based on likelihoods, neural networks and energy flow. All methods look for an enhancement of upward going

multi-ring events. The results indicate a $\sim 2 \sigma$ effect, not statistically significant to claim the observation of $\nu_{\tau s}$.

4 Results from accelerator neutrino experiments

Coming back to sterile neutrinos, the motivation for a 4-neutrino mixing scheme originated from the result of the LSND experiment at the Los Alamos Meson Facility (LAMPF) [16]. The LSND detector was designed to detect neutrinos and to search specifically for $\bar{\nu}_{\mu} \rightarrow \bar{\nu}_e$ and $\nu_{\mu} \rightarrow \nu_e$ oscillations. The neutrino beam is obtained by sending 800 MeV proton pulses with a frequency of 120 Hz onto a water target 30 cm long. The detector consists of a volume of 167 ton of mineral oil viewed by 1220 PMTs. The detector is contained in a steel tank roughly cylindrical in shape and located under 2 kg/cm² of steel overburden to shield it from cosmic rays.

The $\bar{\nu}_{\mu} \rightarrow \bar{\nu}_e$ search has been performed by looking at the appearance of $\bar{\nu}_e$ in the large flux of $\bar{\nu}_{\mu}$ from muon decay at rest (DAR). LSND detects $\bar{\nu}_e$ through the reaction $\bar{\nu}_e p \rightarrow e^+ n$ followed by the neutron-capture reaction $np \rightarrow d\gamma$ (2.2 MeV). Hence, the signature of neutrino oscillation consists of an *electron* signal followed by a 2.2 MeV photon correlated in time and position to the positron. The $\nu_{\mu} \rightarrow \nu_e$ search was accomplished by looking at the appearance of ν_e interactions in a dominant ν_{μ} beam from pions which decay in flight (DIF). A candidate $\nu_{\mu} \rightarrow \nu_e$ event from a DIF ν_{μ} consists of a single and isolated electron with energy in the range $60 < E_e < 200$ MeV produced in the reaction $\nu_e C \rightarrow e^- X$.

The result of the experiment is a positive indication of an oscillation signal with an excess of 83.3 ± 21.2 events (DAR). This signal is corroborated by the DIF analysis and corresponds to an oscillation probability of $(2.6 \pm 0.6 \pm 0.4) \times 10^{-3}$.

A similar experiment (KARMEN) [17] was conducted at the neutron spallation facility ISIS of the Rutherford Appleton Laboratory. The experiment was based on 56 ton of liquid scintillator and was originally designed to study neutrino nucleus interactions. Pions are created in the interaction of 800 MeV protons onto a heavy target ($Ta - D_2O$) and π^- are absorbed by nuclei. Neutrinos are produced by π^+ DAR. The KARMEN neutrino spectrum is similar to that of LSND. The KARMEN experiment, however, profits from the peculiar time structure of the beam. Two parabolic proton pulses of 100 ns base width with a gap of 225 ns are produced with a repetition rate of 50 Hz. The different mean lifetimes of the π (26 ns) and of the μ (2.2 μ s) ensure a clear separation in time of the ν_{μ} burst from the following ν_e and $\bar{\nu}_{\mu}$. Furthermore, due to the heavy target, the ν production region is essentially limited to a region ± 5 cm radial to the proton beam and ± 10 cm along the beam axis. This allows an excellent resolution in the measurement of the baseline. The experiment did not observe any significant excess of events exploring an oscillation parameter region largely overlapping that of the LSND signal.

Due to the controversial LSND and KARMEN results the MiniBoone experiment [18]) is in preparation at Fermilab with the aim of testing the LSND signal with much higher sensitivity. It will exploit a neutrino beam obtained by sending 8 GeV protons accelerated by the Fermilab Booster onto a titanium target. Its

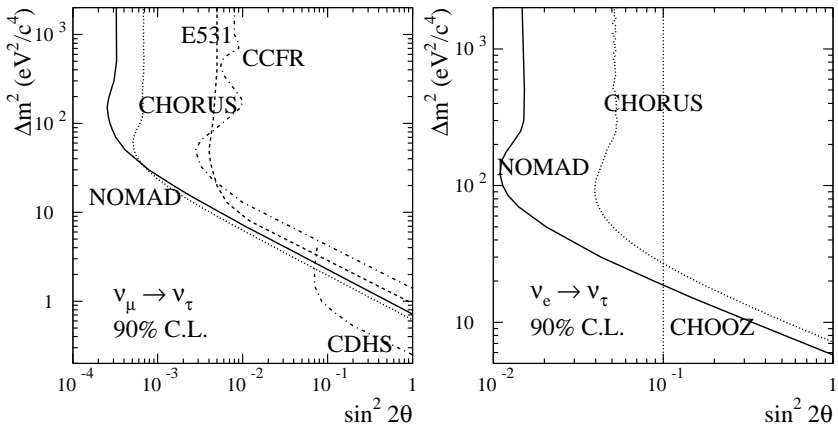


Fig. 4. Exclusion plots of the CHORUS and NOMAD experiments for $\nu_\mu \rightarrow \nu_\tau$ and $\nu_e \rightarrow \nu_\tau$ searches. The analysis of CHORUS is still in progress

goal is to collect ~ 1000 events per year if the LSND signal is due to $\nu_\mu \rightarrow \nu_e$ oscillations. This could allow to establish the evidence for oscillations at the 8 σ level.

Also the search for oscillations carried out by the CERN CHORUS and NOMAD collaborations [2] in the $\nu_\mu \rightarrow \nu_\tau$ channel yielded a negative result. CHORUS and NOMAD were proposed in the early '90s to search for oscillations in the parameter region relevant for the Dark Matter puzzle. Therefore, they were designed to be sensitive to small mixing angles ($\sin^2 2\theta_{\mu\tau} \sim 10^{-4}$) and relatively large Δm^2 ($\mathcal{O}(10 \text{ eV}^2)$). The experiments exploited two complementary approaches in the search for τ s possibly produced in ν_τ charged current interactions. CHORUS used a large mass emulsion target for the direct detection of the short τ track and of its decay topology. NOMAD employed a low density target made of drift chambers placed in a magnetic field for precise reconstruction of the event kinematics. The negative results of the experiments are presented in Fig. 4 for both $\nu_\mu \rightarrow \nu_\tau$ and $\nu_e \rightarrow \nu_\tau$ searches.

Finally, the first LBL neutrino experiment started in 1999 with the commissioning of the K2K [19] beam from KEK to the Super-Kamiokande detector 250 km away [20] with the aim of a ν_μ disappearance search in the parameter region indicated by the atmospheric anomaly. ν_μ s are generated by sending with a fast extraction 12 GeV protons from the K2K Proton Synchrotron onto an aluminum target. The time duration of one spill is 1.1 μs and the spill frequency is 2.2 Hz with a nominal intensity of $\sim 6 \times 10^{12}$ protons/spill. A total of 4.6×10^{19} pot have been extracted until April 2001. The final goal is 10^{20} pot.

Positively charged mesons produced in the target are focused towards Super-Kamiokande by a toroidal magnetic field produced by a pair of horns. The mean energy of the neutrino beam is 1.4 GeV with a peak at 1 GeV. The ν_e contamination has been estimated to be $\sim 1\%$.

Table 2. Results from K2K for different classes of events. Expected event yields come from the 1 *kton* water Cerenkov. Δm^2 is given in units of $10^{-3} eV^2$ and full mixing is assumed

Event type	Expected evts. (no osc.)	Observed evts.	$\Delta m^2 = 3$	$\Delta m^2 = 5$	$\Delta m^2 = 7$
Fully cont.	44	$63.9^{+6.1}_{-6.6}$	41.5	27.4	23.1
1 ring	26	38.4 ± 5.5	22.3	14.1	13.1
μ -like	24	34.9 ± 5.5	19.3	11.6	10.7
e -like	2	3.5 ± 1.4	2.9	2.5	2.4
multi ring	18	25.5 ± 4.3	19.3	13.3	10.0

A ν_μ disappearance experiment is performed by comparing the event rates in several 'near' detectors with those observed in Super-Kamiokande. In particular, a 1 *kton* water Cerenkov completely analogous to Super-Kamiokande is used in order to reduce systematic errors in extrapolating the rate measurement of the 'near' to the 'far' detector.

Events collected in Super-Kamiokande are classified according to the usual scheme (fully contained, partially contained, ...). The predictions from the near detectors agree among them within the experimental uncertainties. From the 1 *kton* water Cerenkov one would expect $63.9^{+6.1}_{-6.6}$ fully contained events in Super-Kamiokande whereas 44 are actually observed. This is consistent with the hypothesis of $\nu_\mu \rightarrow \nu_\tau$ oscillation occurring with the same parameters of the Super-Kamiokande atmospheric neutrino data (Table 2). The probability for the 'no-oscillation' hypothesis is lower than 3%.

Figure 5 shows the reconstructed energy spectrum of the K2K events compared with the expected spectrum in the absence of oscillations. If oscillation occurred with the Super-Kamiokande favored parameter values one would observe the 'disappearance' of ~ 600 MeV neutrinos. Although there are some positive indications the statistical significance is still too small to make any conclusion.

5 Future studies on solar neutrinos

The results from solar neutrino experiments depict a scenario where there is evidence for inclusive appearance of ν_μ or ν_τ from ν_e , the SSM seem to be correct given the measurement of the 8B neutrino flux from the Sun, and where there is no evidence for spectral distortions, day/night effects and seasonal distortions.

The next generation solar neutrino experiments is expected to contribute to the clarification of these issues. SNO will soon perform the measurement of the charged to neutral current event ratio. GNO, SNO and Super-Kamiokande will be able to observe effects that can discriminate between neutrino oscillation schemes, such as day-night and seasonal variations of the solar signal (which are model independent) and spectrum distortion of the recoil electrons from neutrino interactions. In particular, important results are expected in the near future by the BOREXINO [21] and KAMLAND [22] experiments.

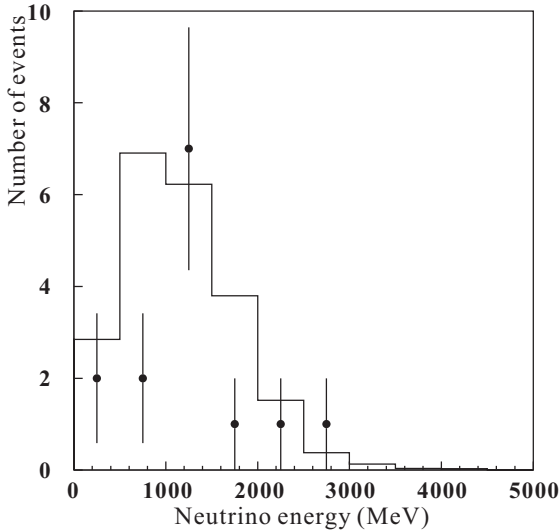


Fig. 5. Observed energy spectrum of K2K events. The continuous line corresponds to the expectations in the absence of oscillations. The deficit in the second bin is consistent with the oscillation parameter values indicated by Super-Kamiokande

The construction of the BOREXINO detector is being completed in the Hall C of the Gran Sasso Laboratory. The main aim of the experiment is the measurement of the solar flux ${}^7\text{Be}$ component, a key ingredient of the Solar Neutrino Problem. BOREXINO will be able to detect these neutrinos by real time counting. The detector consists of a volume of 300 ton of pure liquid scintillator (pseudocumene and PPO) viewed by ~ 2000 PMTs. A steel sphere supports the PMTs and separates the scintillators from an external volume of water used as a veto (Fig. 6).

Solar neutrinos from the ${}^7\text{Be}$ line at 0.862 MeV are detected through the $\nu_e \rightarrow e$ scattering that proceeds via charged and neutral currents unlike ν_μ and ν_τ interactions. ν_e conversion into another flavour would produce a reduction of the detected ${}^7\text{Be}$ flux with respect to the expected one (about 50 per day for 100 ton of scintillator). This reduction can be studied against the MSW solutions (large and small mixing angle), day/night effects (low Δm^2 solution) and seasonal variations (vacuum oscillations).

The KAMLAND experiment will use reactor neutrinos to investigate MSW solutions of the solar neutrino deficit. The detector is placed at the site originally occupied by the Kamiokande detector. It is made of ~ 1000 ton of high purity liquid scintillator housed in a spherical balloon of 13 m diameter viewed by about 2000 PMTs. Electron anti-neutrinos originate mainly from several Japanese commercial reactors located at an average distance of $\sim 150 - 200$ km from the detector and have a mean energy of ~ 3.5 MeV. This corresponds to a L/E interval that allows to probe with high sensitivity the LMA solution of the solar deficit. This is a case rather similar to that of LBL accelerator experiments

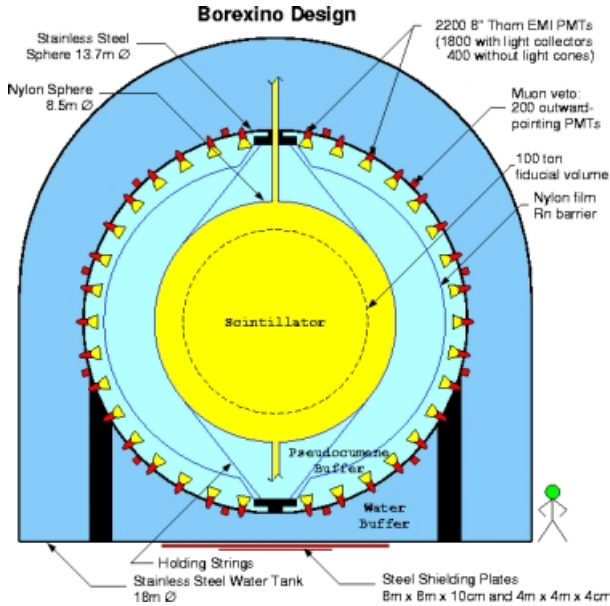


Fig. 6. Schematic view of the BOREXINO detector

which feature L/E ratios compatible with the oscillation parameters indicated by atmospheric neutrino experiments. The sensitivity of KAMLAND is shown in Fig. 7 for a three year run.

KAMLAND will eventually detect also ${}^7\text{Be}$ and ${}^8\text{B}$ neutrinos in a way analogous to BOREXINO. However, while BOREXINO is particularly optimized for the detection of ${}^7\text{Be}$ neutrinos, the larger mass of KAMLAND should allow the measurement of the low energy part of the ${}^8\text{B}$ spectrum, whereas the high energy component will be studied by SNO and Super-Kamiokande.

Finally, one should note that other experimental approaches have been proposed or are being used to further study the most abundant component of the solar neutrino spectrum, *i.e.* pp neutrinos. I wish to mention the idea of the LENS experiment [23], a proposed real time experiment using 20 *ton* of Ytterbium able to perform a direct measurement of pp and ${}^7\text{Be}$ neutrinos with high energy resolution (separation between the two corresponding peaks) and large statistics. About 200 and 150 events induced by pp and ${}^7\text{Be}$ neutrinos, respectively, could be collected per year.

6 Atmospheric neutrino detectors and LBL experiments

More studies on the atmospheric neutrino deficit could be pursued by a new generation of atmospheric neutrino detectors able to pin down the oscillation pattern as a function of L/E , and by LBL experiments able to probe the small Δm^2 values favored by the existing data, following the pioneering K2K experiment. The two approaches are to be considered complementary, both in relation

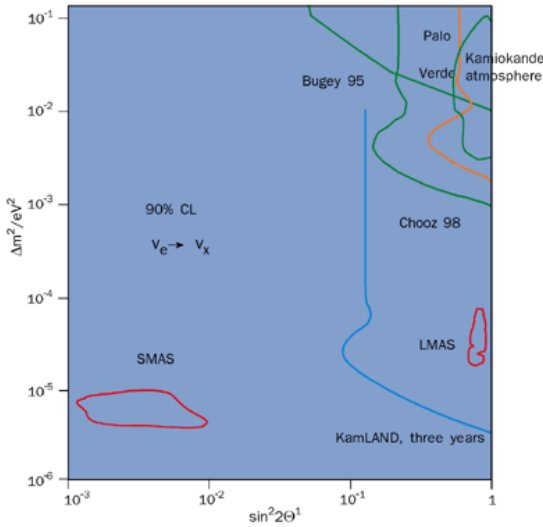


Fig. 7. The sensitivity curve of KAMLAND compared with oscillation solutions of the Solar Neutrino Problem. The LMA solution parameters will be explored by the experiment

to the oscillation parameter regions that they explore and to the experimental methods which are employed. This is presented in Fig. 8, where the spectra of atmospheric and LBL neutrinos are shown as a function of L/E and are compared to the oscillation probability derived by the Super-Kamiokande results.

An example of a proposed atmospheric neutrino detector capable to 'see' the oscillation pattern is MONOLITH [24]. It consists of a ~ 30 kton magnetized iron spectrometer ($B = 1.3$ T) made of 8 cm thick iron plates inter-spaced with glass RPCs and complemented by scintillator veto detectors. The experiment is designed to run underground and exploits the up/down symmetry of the high energy (above 2 GeV) component of the atmospheric neutrino flux. The oscillation pattern can then be observed by plotting the ratio between upward-going and downward-going muons as a function of L/E (Fig. 9). The experiment is mostly sensitive to values of Δm^2 below a few $10^{-3} eV^2$, a region where LBL experiments lose their sensitivity.

Concerning LBL projects, three facilities have been approved and will start operation in a few years. The MINOS experiment [25] in the USA starting from 2005 will use the NuMI beam [26] from the Fermilab Main Injector to test the hypothesis of neutrino oscillation with $\Delta m^2 \sim 10^{-2} - 10^{-3} eV^2$. Neutrinos have a relatively low energy (from 3 to 15 GeV) optimized for a ν_μ disappearance search. Two detectors are placed in a near (at ~ 1 km distance from the source) and a far location (in the Soudan mine 730 km away from Fermilab), respectively. The far detector consists of two super-modules each made of magnetized iron toroids inter-spaced by scintillating strip detectors read out by multi-anode PMTs. The mass of each super-module is about 2.7 kton and the magnetic field has an

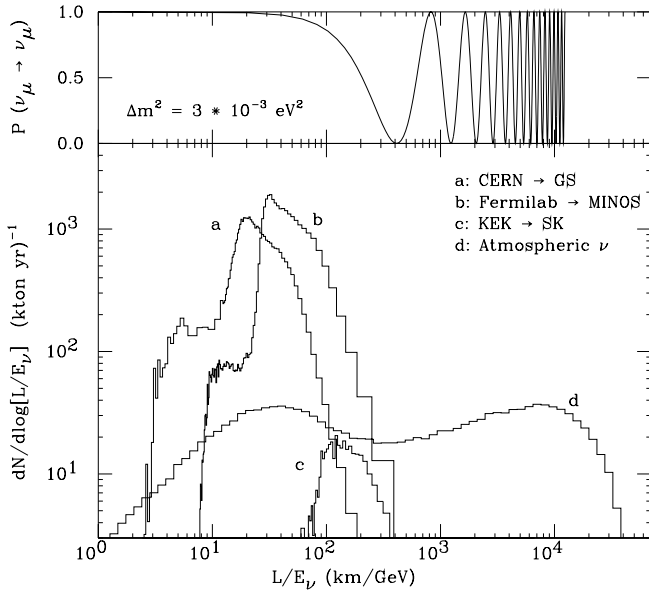


Fig. 8. Top curve: ν_μ survival probability for $\Delta m^2 = 3 \times 10^{-3} eV^2$; bottom: ν_μ charged current spectra for LBL beams and atmospheric neutrinos

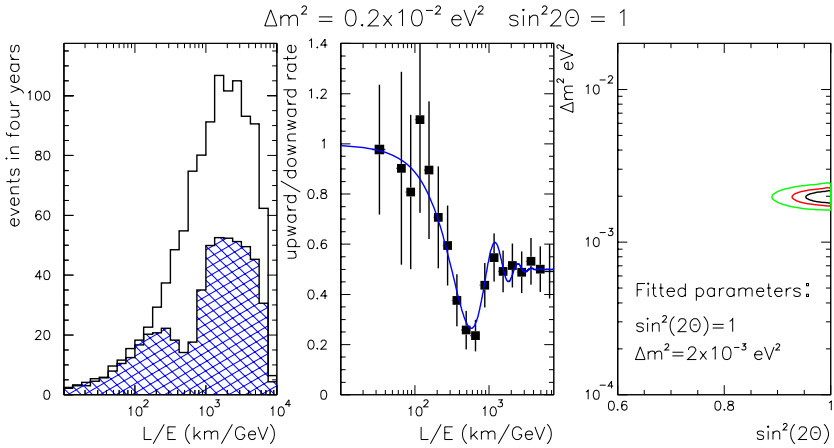


Fig. 9. Expected results from MONOLITH

intensity of 1.5 T . Oscillations are detected by comparing the yields of 'long' events with penetrating tracks due to muons (ν_μ induced charged currents) and 'short' events (neutral currents from ν_μ, ν_e and ν_τ as well as charged currents from ν_e and ν_τ) in both the near and far detectors. The design sensitivity of MINOS is shown in Fig. 10 together with the Super-Kamiokande signal.

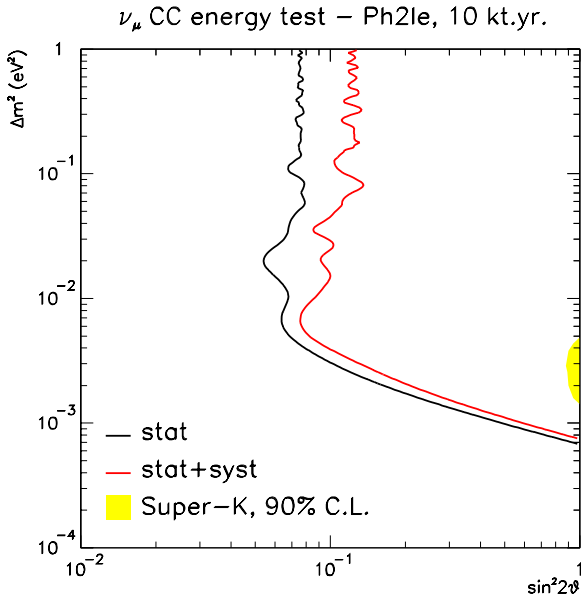


Fig. 10. Sensitivity curves for MINOS ($\nu_\mu \rightarrow \nu_\tau$ search)

In Europe, the CNGS beam [27] from CERN to Gran Sasso will also be commissioned in 2005. Differently from NuMI it has been optimized for LBL experiments (OPERA [3] and ICARUS [28]) with the aim of an appearance search for $\nu_\mu \rightarrow \nu_\tau$ oscillation. For this reason no near detector is needed and the neutrino energy is higher than for NuMI (~ 20 GeV). The baseline is also in this case ~ 730 km. A schematic layout of the underground structures of the facility is shown in Fig. 11.

Two complementary τ detection methods are adopted by OPERA and ICARUS. OPERA exploits the emulsion technique (similarly to DONUT) for the direct observation of the short τ track. The detector is based on the Emulsion Cloud Chamber (ECC) concept which combines the high precision tracking capabilities of nuclear emulsions and the large mass achievable by employing metal plates as a target. The ECC is a detector made of a sandwich of lead plates inter-spaced with nuclear emulsion films ($300 \mu\text{m}$ thick) used as high precision tracking devices. This detection technique combined with the availability of automatic emulsion scanning devices allows to conceive and realize a large mass fine-grained vertex detector for the direct identification of ν_τ appearance.

If a τ is produced by a ν_τ interacting in a lead plate it will decay and will be detected by measuring the angle between the charged decay daughter and the τ direction. This kink angle is caused by the invisible neutrino(s) produced in the decay. For its measurement the directions of the tracks before and after the kink are reconstructed in space by means of a pair of emulsion films sandwiching the lead plate where the primary vertex occurred (Fig. 12). All τ decay modes are considered in OPERA. The electron channel, in particular, benefits from the



Fig. 11. Underground layout of the CNGS neutrino beam from CERN to Gran Sasso

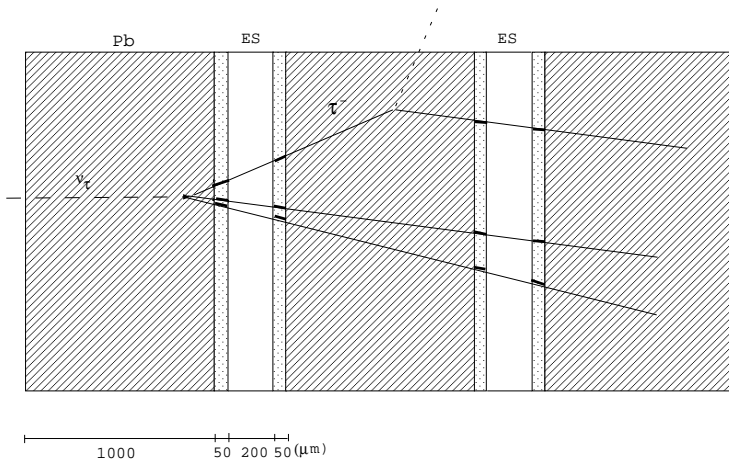


Fig. 12. Schematic structure of the OPERA target consisting of a sandwich of thin emulsion films and lead plates. The τ decay kink is directly reconstructed in space by using four track segments in the films

dense lead-emulsion sandwich structure which allows the electron identification through its showering in the downstream cells.

By piling up emulsion films and lead plates in a sandwich-like structure one obtains the so-called *brick* which constitutes a detector element appropriate for the assembly in planar matrix structures (*walls*). The total target mass of ~ 2000 ton is obtained with about 230000 bricks. The ECC target is complemented by electronic detectors. In particular, planes of scintillator strips placed downstream of each emulsion brick wall, have the task to identify the brick where the neutrino interaction took place and to guide the scanning, so providing time resolution to the emulsions.

Once the *fired* brick has been identified it is removed from the detector and its emulsions are developed and scanned by means of automatic high-speed microscopes. Starting from the most downstream emulsion film in the brick, track segments are detected and measured in position and angle. This procedure continues in the other films until the interaction vertex plate is found. The search for a decay topology is then performed by looking in the brick volume around the primary vertex.

Thanks to the direct τ detection OPERA is characterized by a low expected background. About 12 signal events with a background of 0.7 would be observed if oscillations occur with parameter values corresponding to the present Super-Kamiokande best fit.

ICARUS exploits the bubble-chamber like space resolution of a liquid argon TPC for a detailed kinematical reconstruction of the events. The working principle of the detector is simple. A large liquid argon volume is contained in a cryostat equipped with two readout wire-planes (one at each end of the volume) and a high voltage plane at the center giving a long drift length. Ionization electrons produced by charged particles crossing the liquid argon are collected at the readout planes. The arrival time of the different electrons allows the reconstruction of the particle track trajectory by the time projection technique. Each readout plane has three coordinates at 60° from each other and wire pitch of 3 mm. This corresponds to a *bubble* diameter of about 3 mm, of the same order of the bubble size of the Gargamelle detector at CERN.

The detector is a homogeneous tracking device capable of dE/dx measurement. Its high dE/dx resolution allows good momentum measurement and particle identification of soft particles. Electromagnetic and hadronic showers are, in fact, fully sampled. This gives good energy resolution for electromagnetic and hadronic contained showers and excellent electron identification and e/π^0 separation.

A full size large module of 600 ton has been recently constructed and tested with cosmic rays. It will eventually be installed in the Gran Sasso Laboratory and represents the basic unit to build-up the required detector mass of about 2500 ton. Fig. 13 displays one event with an electron induced by cosmic rays showering in the prototype volume. One can see the excellent space resolution and electron identification capability of the detector. The sensitivity of the experiment in searching for $\nu_\mu \rightarrow \nu_\tau$ oscillation in the CNGS beam is similar to the one of OPERA, covering the Super-Kamiokande preferred parameter values. In its final configuration ICARUS will be a rather general purpose detector capable

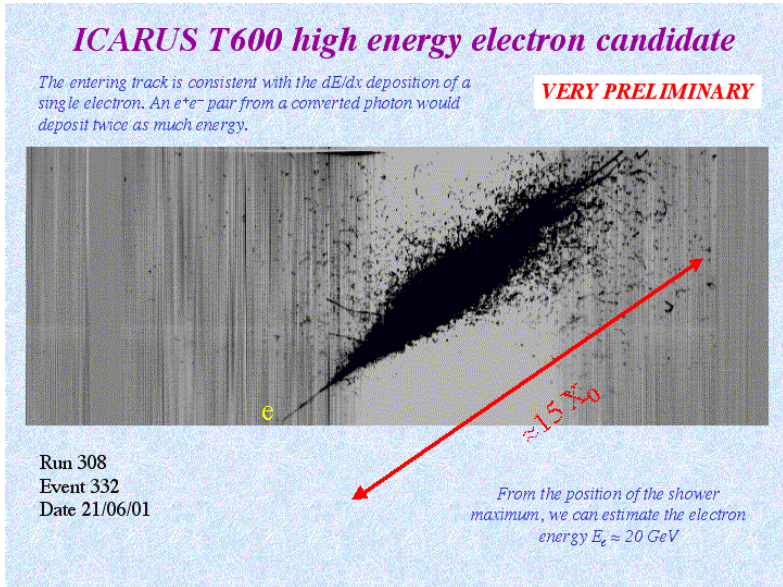


Fig. 13. An electron event (induced by cosmics) collected with the ICARUS 600 ton prototype

of performing with high sensitivity experiments on proton decay as well as on solar and atmospheric neutrinos.

A third LBL neutrino beam will be obtained from the future high intensity Japan Hadron Facility (JHF) and will be commissioned in 2007 and will run from Jaeri to Kamioka (at 295 km distance) [2]. The beam features high intensity (10^{21} protons per year) and low neutrino energy ($\sim 1 \text{ GeV}$). A ν_μ disappearance search can be performed by means of the existing Super-Kamiokande detector. In a second phase one foresees a factor 200 increase in intensity and the use of the proposed Hyper-K megaton detector, follow-up of Super-Kamiokande.

7 Coming next: Study of the mixing matrix

After the running or planned LBL experiments with neutrino beams from meson decay and of solar neutrino experiments such as GNO, KAMLAND and BOREXINO, a much more clear picture of neutrino mixing will likely emerge. My 'preferred' scenario, as an experimentalist, is the one where oscillations will be confirmed for both solar (LMA solution!) and atmospheric ('large' Δm^2) neutrinos with parameters measured within 10%, and with the LSND result not due to oscillations (three flavor mixing matrix without sterile neutrino). In that scheme, the mixing among three neutrino families can be written as

$$\begin{pmatrix} \nu_e \\ \nu_\mu \\ \nu_\tau \end{pmatrix} = U_{\alpha i} \begin{pmatrix} \nu_1 \\ \nu_2 \\ \nu_3 \end{pmatrix}$$

The 3×3 unitary mixing matrix U is described by

$$U = \begin{pmatrix} c_{12}c_{13} & s_{12}c_{13} & s_{13}e^{-i\delta} \\ -s_{12}c_{23} - c_{12}s_{23}s_{13}e^{i\delta} & c_{12}c_{23} - s_{12}s_{23}s_{13}e^{i\delta} & s_{13}c_{13} \\ s_{12}s_{23} - c_{12}c_{23}s_{13}e^{i\delta} & -c_{12}s_{23} - s_{12}c_{23}s_{13}e^{i\delta} & c_{23}c_{13} \end{pmatrix}$$

where $c_{ij} = \cos\theta_{ij}$, $s_{ij} = \sin\theta_{ij}$ and δ is the CP violating phase. Neutrino oscillation can be expressed in terms of six independent variables $\Delta m_{21}^2 = |m_2^2 - m_1^2|$, $\Delta m_{31}^2 = |m_3^2 - m_1^2|$, θ_{12} , θ_{13} , θ_{23} and δ .

In the general framework of a three-flavor mixing scheme and under the assumption of a hierarchical mass spectrum $m_1 < m_2 \ll m_3$ ($\Delta m_{23}^2 > 0$), the largest Δm^2 corresponds to the atmospheric neutrino deficit. One has then 5

$$U = \begin{pmatrix} 1 & 0 & 0 \\ 0 & c_{23} & s_{23} \\ 0 & -s_{23} & c_{23} \end{pmatrix} \begin{pmatrix} c_{13} & 0 & s_{13} \\ 0 & 1 & 0 \\ -s_{13} & 0 & c_{13} \end{pmatrix} \begin{pmatrix} c_{12} & s_{12} & 0 \\ -s_{12} & c_{12} & 0 \\ 0 & 0 & 1 \end{pmatrix}$$

where the first matrix refers to atmospheric and the third to solar neutrinos, respectively.

Terrestrial neutrino oscillation experiments can be sensitive to the oscillation parameters through the measurement of the probabilities

$$P(\nu_\mu \rightarrow \nu_e) \simeq \sin^2 2\theta_{13} \sin^2(\theta_{23}) \sin^2 \frac{\Delta m_{23}^2 L}{4E}$$

$$P(\nu_e \rightarrow \nu_\tau) \simeq \sin^2 2\theta_{13} \cos^2(\theta_{23}) \sin^2 \frac{\Delta m_{23}^2 L}{4E}$$

$$P(\nu_\mu \rightarrow \nu_\tau) \simeq \sin^2 2\theta_{23} \cos^4(\theta_{13}) \sin^2 \frac{\Delta m_{23}^2 L}{4E}$$

From the above relations it turns out that the measurement of the oscillation probabilities $P(\nu_\mu \rightarrow \nu_e)$ and $P(\nu_e \rightarrow \nu_\tau)$ allows to determine the $\sin^2 2\theta_{13}$ mixing parameter. At present, only an upper limit of about 0.1 exists on $\sin^2 2\theta_{13}$, as derived by the CHOOZ experiment. A fit to their data yields $\sin^2 2\theta_{13} \simeq 0.05$ [29]. Concerning future measurements of $\sin^2 2\theta_{13}$ we note that electron detection is easier than τ detection. This favors ν_e appearance experiments that can be performed with LBL conventional beams or with reactors, and atmospheric neutrino experiments searching for MSW effects. The above experiments, however, are severely limited by background and need long runs to collect an adequate statistics.

The hypothesis of $\Delta m_{23}^2 > 0$ can be tested by searching for oscillation of neutrinos traveling through the Earth matter (MSW effect). In that case the above oscillation probability relations are modified and become function of the three mixing angles in vacuum (θ_{12} , θ_{13} and θ_{23}), of the vacuum mass differences squared (Δm_{12}^2 and Δm_{23}^2), of the baseline L , of the neutrino energy E and of the average Earth density along the path ρ .

Possible effects indicating CP violations in the leptonic sector are expected to be small. They can be detected by comparing the oscillation probabilities

which involve neutrinos and anti-neutrinos, respectively. Under the approximation $|\Delta m_{23}^2| \gg |\Delta m_{12}^2|$, one can define the asymmetry

$$A_{CP} = \frac{P(\nu_e \rightarrow \nu_\mu) - P(\bar{\nu}_e \rightarrow \bar{\nu}_\mu)}{P(\nu_e \rightarrow \nu_\mu) + P(\bar{\nu}_e \rightarrow \bar{\nu}_\mu)} \propto \frac{\sin 2\theta_{12}}{\sin \theta_{13}} \sin \delta \sin \frac{\Delta m_{12}^2 L}{4E}$$

The effect is maximal for $\delta = \pm\pi/2$ and vanishes for $\delta = 0$. In order to have an experimentally detectable A_{CP} , Δm_{12}^2 and $\sin 2\theta_{12}$ must be 'large'. This requirement implies that the solar LMA solution must hold. Moreover, since $P(\nu_\mu \rightarrow \nu_e) \propto \sin^2 2\theta_{13}$ and $A_{CP} \propto 1/\sin \theta_{13}$ a small value of $\sin^2 2\theta_{13}$ implies low statistics and large asymmetry, whereas a large $\sin^2 2\theta_{13}$ value gives high statistics but low asymmetry. These last considerations obviously have an impact on the detector design. Last but not least, conventional beams are certainly not adequate to the measurement of CP violating effects. In fact, since

$$P(\nu_\mu \rightarrow \nu_e) \propto \sin^2 \frac{\Delta m_{23}^2 L}{4E}$$

oscillations are governed by Δm_{atm}^2 , L and E . For a neutrino beam of $\sim 15 \text{ GeV}$ a long baseline of $\simeq 10000 \text{ km}$ is required with a consequent too low neutrino flux and, hence, event statistics.

From all the above consideration it emerges the need for a new generation experiments for precision tests of the neutrino mixing matrix exploiting non conventional high-intensity neutrino beams from meson decay (super-beams) or from muon decay (neutrino factories).

8 Super-beams and neutrino factories

Super-beams can be considered as a first step before the construction of a neutrino factory. High intensity proton drivers are used to provide high neutrino-parent fluxes. Some designs exist of intense low-energy neutrino facilities suitable for ν_μ disappearance experiments. In its first phase the already mentioned JHF beam will run with a 0.77 MW proton beam eventually upgraded to 4 MW . Other laboratories equipped with high intensity drivers could envisage the construction of neutrino super-beams. In particular, a 1.6 MW proton driver is under study at Fermilab and a $4 \text{ MW-}2 \text{ GeV}$ linac is being considered at CERN for a LBL ($\sim 150 \text{ km}$) experiment.

However, neutrino factories will likely provide the best opportunity for oscillation physics, producing beams containing either high energy electron neutrinos and muon anti-neutrinos or electron anti-neutrinos and muon neutrinos, according to the polarity of the decaying muons. This purely leptonic process allows to get rid of the uncertainties related to hadronic reactions which are relevant in the case of neutrino beams from pion decays. Therefore, fluxes can be easily predicted. Moreover, one has the freedom of choosing the neutrino spectrum by fixing the storage ring energy. From the decay chains $\mu^- \rightarrow e^- \nu_\mu \bar{\nu}_e$ and $\mu^+ \rightarrow e^+ \nu_e \bar{\nu}_\mu$ an equal number of ν_e ($\bar{\nu}_e$) and $\bar{\nu}_\mu$ (ν_μ) populate the beam, contrary to the case of beams from pion decay.

A description of the general features of such beams and reports about feasibility studies can be found in [30]. Muons are allowed to decay in one of the straight sections of the storage ring. The neutrino energy and angular distributions are functions of the parent muon energy, of the decay angle and of the muon spin direction. The neutrino beam intensity can be orders of magnitude higher than that of conventional beams. It depends on the rate at which muons are stored in the ring and hence on the muon source. The source can consist of a proton accelerator, a target for the production of pions, a focusing system, a decay channel and a muon cooling section. Preliminary studies on neutrino sources from muon storage rings have been performed and the possible use of the existing accelerator facilities in Europe, Japan and USA was considered. One expects to produce more than 10^{20} neutrinos (or anti-neutrinos) per year. This implies, for example, that under the assumption of 20 GeV unpolarized muons, of absence of neutrino oscillation and of a site 10000 km away from the source (e.g. as for a beam from Fermilab to Super-Kamiokande) one could obtain $\sim 2.2 \times 10^{20} \bar{\nu}_\mu m^{-2}$ per year and the same number of ν_e .

LBL experiments placed at distances ranging from ~ 1000 to ~ 10000 km from the source of muon decay beams will consolidate the knowledge of neutrino mixing and will also allow to start a complete program of neutrino oscillation physics in a general three-flavor mixing scheme. Additional physics subjects could be the detection of Earth matter effects and possible CP and T violation in the leptonic sector. This will be accomplished by means of the intense neutrino and anti-neutrino beams which could be obtained by changing the polarity of the stored muons.

The availability of high intensity neutrino beams with well known composition will allow to detect all appearance channels ($\nu_e \rightarrow \nu_\mu$, $\bar{\nu}_e \rightarrow \bar{\nu}_\mu$, $\nu_e \rightarrow \nu_\tau$, $\bar{\nu}_e \rightarrow \bar{\nu}_\tau$, $\nu_\mu \rightarrow \nu_\tau$ and $\bar{\nu}_\mu \rightarrow \bar{\nu}_\tau$). In particular, the ν_e component of the beam is essential ingredient for the measurement of the oscillation parameters in the three-flavor mixing, of tests of the MSW effect and of CP violating effects.

In general, the outcome of the planned neutrino program will drive the future experimental explorations at the neutrino factories and hence the design features of the facilities and of the experiments.

9 Visionary conclusions...

My talk at this Symposium took place in the concluding 'visionary session'. Therefore, in the spirit of the organizers, I intend to give (at least) some visionary conclusions by partially reporting what was (...will be) said by Carlo Rubbia III in his concluding remarks of Neutrino42, held in Capri in 2042:

"I will start this review from 2002. Incidentally, you may remember that in that year Roger Cashmore found the bright solution to the problem of the LHC cost overrun.... Also in 2002 the first results from Kamland proved that the LMA solution of the Solar Neutrino Deficit is the correct one. Two years later the Collaboration measured $\Delta m_{12}^2 = (8.56 \pm 0.2) \times 10^{-5} eV^2$ and $\sin^2 2\theta_{12}$ compatible with 1, within 4%.

Although expected by indications from phenomenological fits, MiniBoone presented at Neutrino04 its final result proving that three neutrinos are enough.

Only some irreducible theoreticians continued talking about sterile neutrinos for a few more years. Concerning atmospheric neutrinos, K2K confirmed (already in 2003) the parameter values indicated by Super-Kamiokande, publishing $\Delta m_{23}^2 = (3.1 \pm 1.1) \times 10^{-3} \text{eV}^2$ and full mixing. This result was very welcome by the LBL community (MINOS, OPERA and ICARUS, the latter led by my great-grandfather).

In fact, in 2006 the first τ 's were seen by OPERA. A paper was published just one week before those reporting analogous oscillation signals from MINOS and ICARUS. The relatively high value of Δm_{23}^2 permitted to measure in two years the oscillation parameters $\Delta m_{23}^2 = (3.3 \pm 0.3) \times 10^{-3} \text{eV}^2$ and $\sin^2 2\theta_{23} = 0.98 \pm 0.04$ (world average). The study of atmospheric neutrinos performed with the Megaton, magnetized UNOLITH calorimeter (jointly built in New Mexico by the former MONOLITH and UNO Collaborations) led in 2010 to the measurement of the sign (positive!) of Δm_{23}^2 by comparing the resonant matter effects in neutrino and anti-neutrinos. This occurred exactly two years after the discovery of the 118 GeV Higgs by ATLAS and CMS.

JHF went smoothly in operation and in 2012 the HyperK Collaboration measured the relatively large value of 2.5% for $\sin^2 2\theta_{13}$. The fortunate combination of large $\sin^2 2\theta_{13}$, Δm_{12}^2 and $\sin^2 2\theta_{12}$ motivated and justified the continuing effort for the WNF (World Neutrino Factory). The goal was to finally detect CP violating effects in the neutrino sector. The machine was commissioned in 2016 at Brookhaven and the two beams were sent to HyperK and Gran Sasso. At LNGS, the 50 kton magnetized OPERA III emulsion detector was installed in the recently excavated Hall D with the aim of studying wrong sign muon events with τ tagging capabilities, an approach complementary to that of the upgraded 100 kton ICARUS IV detector.

The era of precision studies of the neutrino mixing matrix elements started. The CP violating phase was measured a few years later together with all the transitions including $\nu_e \rightarrow \nu_\tau$. But as you well know, neutrinos did not finish to bring unexpected results: in 2025 the signal from Super-Amanda opened the Non Standard Frontier. Since then a new era started: I have today the impossible task to summarize the many achievements of these last 17 years..."

Acknowledgements. I wish to warmly thank the organizers of the LHC 2001 Symposium and in particular Profs. R. Cashmore and B. Saitta for the kind invitation. I am also indebted to Lucio Ludovici for supplying me material and smart suggestions.

References

1. Ch. Weinheimer et al., Phys. Lett. B 460 (1999) 219; V.M. Lobashev et al., Phys. Lett. B 460 (1999) 227.
2. S. Aoki, Proc. of the Lepton Photon 2001 Conference, Rome, 23-28 July 2001.
3. OPERA web page: <http://operaweb.web.cern.ch/operaweb/index.shtml>.
4. J. Goodman, Proc. of the Lepton Photon 2001 Conference, Rome, 23-28 July 2001.
5. J.N. Bahcall et al., Phys. Rev. Lett. 20 (1968) 1209; J.N. Bahcall et al., Phys. Lett. B 433 (1998) 1; [http://www.sns.ias.edu/~sim\\$jb/](http://www.sns.ias.edu/~sim$jb/).

6. J. Klein, Proc. of the Lepton Photon 2001 Conference, Rome, 23-28 July 2001.
7. R. Davis Jr. et al., Phys. Rev. Lett. 20 (1968) 1205.
8. W. Hampel et al., Phys. Lett. B 447 (1999) 127; M. Altmann et al., contrib. paper at the XIX Int. Conf. on Neutrino Phys. and Astroph., Sudbury, 2000.
9. J. N. Adburashitov et al., Phys. Rev. C 60 (1999) 055801.
10. S.P. Mikheyev and A.Yu. Smirnov, Yad. Fiz. 42 (1985) 1441; L. Wolfenstein, Phys. Rev. D 17 (1985) 2369.
11. G.L. Fogli et al., hep-ph/0106247.
12. M. Honda et al., Phys. Lett. D 52 (1995) 4985; T.K. Gaisser et al., Phys. Lett. D 54 (1996) 5578.
13. M. Apollonio et al., Phys. Lett. B420 (1998) 397; M. Apollonio et al., Phys. Lett. B466 (1999) 415.
14. T. Mann, Proc. of the XIX Int. Conf. on Neutrino Phys. and Astroph., Sudbury, 2000;
15. B. Barish, Proc. of the XIX Int. Conf. on Neutrino Phys. and Astroph., Sudbury, 2000.
16. G. Mills, Proc. of the XIX Int. Conf. on Neutrino Phys. and Astroph., Sudbury, 2000.
17. KARMEN web page: http://www-ik1.fzk.de/www/karmen/karmen_e.html.
18. MiniBoone web page: <http://www-boone.fnal.gov/>.
19. H. Noumi et al., Nucl. Instr. and Meth. A398 (1997) 399.
20. C.K. Jung, Proc. of the Lepton Photon 2001 Conference, Rome, 23-28 July 2001.
21. BOREXINO web page: <http://borex.mi.infn.it>.
22. KAMLAND web page:
<http://www.awa.tohoku.ac.jp/html/KamLAND/index.html>.
23. LENS web page: <http://lens.in2p3.fr/>.
24. MONOLITH web page: <http://castore.mi.infn.it/~monolith/>.
25. MINOS web page: <http://www-numi.fnal.gov:8875/>.
26. The Fermilab NuMI Group, Fermilab Report NuMI-346, October 1998.
27. G. Acquistapace et al., CERN 98-02, INFN/AE-98/05, 19 May 1998; R. Bailey et al., CERN-SL/99-034; INFN/AE-99/05.
28. ICARUS web page: <http://www.aquila.infn.it/icarus/>.
29. G.L. Fogli et al., Phys. Rev. D 59 (1999) 033001.
30. S. Geer, Phys. Rev. D 57 (1998) 6989; V. Barger et al., Phys. Rev. D 61 (2000) 053004; B. Autin, Proc. of the Muon Collider Coll. Workshop, St. Croix, 1999; D. Finley et al., FERMILAB-TM-2072, 1999; A. Blondel et al., CERN Preprint, CERN-EP/2000-53, 2000.